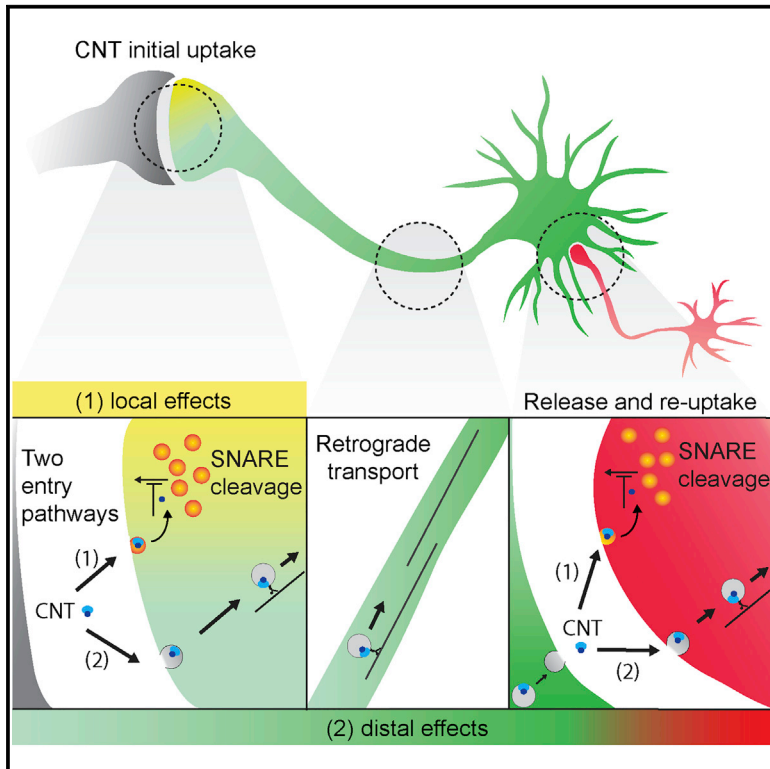**Article**

# Interneuronal Transfer and Distal Action of Tetanus Toxin and Botulinum Neurotoxins A and D in Central Neurons

## Graphical Abstract



## Authors

Ewa Bomba-Warczak, Jason D. Vevea, Joel M. Brittain, ..., Eric A. Johnson, Felix L. Yeh, Edwin R. Chapman

## Correspondence

chapman@wisc.edu

## In Brief

Bomba-Warczak et al. demonstrate that BoNT/A, BoNT/D, and TeNT enter neurons via two separate entry pathways, a canonical synaptic vesicle recycling pathway that leads to local effects and a distinct secondary uptake pathway that directs these toxins to a common, non-acidified, retrograde carrier. This secondary pathway leads to distal effects in neurons upstream from the cells that mediate the initial uptake of these agents.

## Highlights

- BoNT/A, BoNT/D, and TeNT enter neurons via two distinct pathways

- Toxins undergo interneuronal transfer to affect networks of neurons

- Microfluidic devices provide an amenable system to study toxin trafficking

**CellPress**

OPEN ACCESS

Cell Reports
# Article

CellPress

# Interneuronal Transfer and Distal Action of Tetanus Toxin and Botulinum Neurotoxins A and D in Central Neurons

Ewa Bomba-Warczak,[1] Jason D. Vevea,[1] Joel M. Brittain,[1] Annette Figueroa-Bernier,[1] William H. Tepp,[2] Eric A. Johnson,[2] Felix L. Yeh,[3] and Edwin R. Chapman[1],*
[1]Howard Hughes Medical Institute and Department of Neuroscience, University of Wisconsin, Madison, WI 53705, USA
[2]Department of Bacteriology, University of Wisconsin, Madison, WI 53706, USA
[3]Department of Neuroscience, Genentech Inc., South San Francisco, CA 94080, USA
*Correspondence: chapman@wisc.edu
http://dx.doi.org/10.1016/j.celrep.2016.06.104

## SUMMARY

**Recent reports suggest that botulinum neurotoxin (BoNT) A, which is widely used clinically to inhibit neurotransmission, can spread within networks of neurons to have distal effects, but this remains controversial. Moreover, it is not known whether other members of this toxin family are transferred between neurons. Here, we investigate the potential distal effects of BoNT/A, BoNT/D, and tetanus toxin (TeNT), using central neurons grown in microfluidic devices. Toxins acted upon the neurons that mediated initial entry, but all three toxins were also taken up, via an alternative pathway, into non-acidified organelles that mediated retrograde transport to the somato-dendritic compartment. Toxins were then released into the media, where they entered and exerted their effects upon upstream neurons. These findings directly demonstrate that these agents undergo transcytosis and interneuronal transfer in an active form, resulting in long-distance effects.**

## INTRODUCTION

The clostridial neurotoxins (CNTs), comprising tetanus toxin (TeNT) and seven serologically distinct botulinum neurotoxins (BoNT/A–BoNT/G), are among the deadliest agents known, with BoNT/A having an estimated median lethal dose ($LD_{50}$) of 1 ng/kg body weight (Gill, 1982). Due to the potential use of BoNTs as biological weapons, the Centers for Disease Control and Prevention (CDC) designated the BoNTs as tier 1 select agents. Paradoxically, BoNT/A (onabotulinumtoxin A, abobotulinumtoxin A, incobotulinumtoxin A) and BoNT/B (rimabotulinumtoxinB), are also used clinically. In addition to the well-known cosmetic uses of BoNT/A, both serotypes are also used to treat numerous medical conditions, including cervical dystonia, strabismus, migraine headaches, overactive bladder (neurogenic and idiopathic), hyperhidrosis, upper limb spasticity, and blepharospasm (de Maio, 2008). They are also used "off label"

to treat a variety of additional conditions that include chronic lower back pain, traumatic brain injury, cerebral palsy, achalasia, voice abnormalities, and various additional dystonias (Scott, 1980; Schantz and Johnson, 1992; Silberstein et al., 2000; Foster et al., 2001; Jankovic, 1994). According to Allergan's 2013 Annual Report (http://www.allergan.com/miscellaneous-pages/allergan-pdf-files/2013annualreport), more than half of all patients who receive toxin injections do so for medical, rather than aesthetic, reasons. Given their extreme potency, widespread medical use, and potential use as bioterrorism agents, the CNTs are the subject of intensive investigation.

The CNTs are produced by anaerobic, spore-forming bacteria of the genus *Clostridium* (Popoff and Bouvet, 2013). Each CNT is composed of a heavy chain (HC) and a light chain (LC) linked via a disulfide bond. The first step in the action of these agents involves high-affinity interactions with neurons, mediated by their HCs. Binding occurs via a dual-receptor mechanism, where the receptors are composed of polysialic gangliosides in conjunction with proteins. For most of these toxins, protein receptors are presented by recycling synaptic vesicles (SVs). Upon exocytosis, the luminal domains of SV proteins are exposed to the extracellular milieu; BoNT/B, BoNT/G, and a naturally occurring D-C chimera bind to the intraluminal tail of the SV proteins synaptotagmin 1 and 2 (Nishiki et al., 1994; Dong et al., 2003; Rummel et al., 2007; Peng et al., 2012), while BoNTs A, D, and E and TeNT bind to synaptic vesicle protein 2 (SV2) (Dong et al., 2006, 2008; Yeh et al., 2010; Mahrhold et al., 2006, 2013; Peng et al., 2011; Fu et al., 2009; Rummel et al., 2009; Benoit et al., 2014; Yao et al., 2016). BoNT/F was also found to bind to SV2; however, it is not clear whether SV2 serves as a functional protein receptor for this toxin, as primary hippocampal neurons lacking SV2 show no changes in sensitivity to BoNT/F (Fu et al., 2009; Rummel et al., 2009; Peng et al., 2012; Yeh et al., 2010). The identity of the protein receptor for BoNT/C remains to be established. Upon SV endocytosis, the drop in luminal pH triggers the transformation of the HC into a translocation machine (Fischer, 2013; Montal, 2010; Williamson and Neale, 1994; Fu et al., 2002; Puhar et al., 2004; Galloux et al., 2008; Pirazzini et al., 2013); interestingly, the ability to sense low pH requires the interaction of the HC with the ganglioside co-receptor (Sun et al., 2011). The HC then translocates the LC into the cytosol, where it cleaves neuronal soluble

*N*-ethylmaleimide attachment receptors (SNAREs), which form the core of a conserved membrane fusion complex (Rothman, 1994). Cleavage, thereby, inhibits neurotransmission. BoNT/C cleaves the target membrane SNAREs syntaxin and SNAP-25; BoNT/A and BoNT/E cleave SNAP-25; and BoNTs D, B, F, and G and TeNT cleave the vesicular SNARE, synaptobrevin/VAMP (Rossetto et al., 2014; Schiavo et al., 2000; Jahn and Niemann, 1994; Montecucco and Schiavo, 1995). Recently, two additional putative toxin receptors have been identified: fibroblast growth factor receptor 3 (FGFR3) for BoNT/A and nidogens 1 and 2 for TeNT (Bercsenyi et al., 2014; Jacky et al., 2013). How these proteins act in conjunction with the primary protein receptor, SV2, remains unknown.

It is widely believed that BoNT/A confers its medicinal effects by inhibiting synaptic transmission near the site of injection; i.e., that this toxin has only local effects at the neuromuscular junction (NMJ), resulting in flaccid paralysis. However, this idea has been called into question by physicians utilizing this agent in human patients. For example, after peripheral injection of BoNT/A, reciprocal inhibition between agonist and antagonist muscles has been reported, raising the possibility that BoNT/A moves within networks of neurons to affect circuit function (Priori et al., 1995; Aymard et al., 2013; Marchand-Pauvert et al., 2013; Ceballos-Baumann et al., 1997; Giladi, 1997). Alternatively, the observed effects might be due to the compensatory reorganization and remodeling of neuronal networks upstream of the injection site, as a result of purely local effects on the initial uptake neurons (Berardelli and Curra, 2002; Currà et al., 2004; Gilio et al., 2000; Boroojerdi et al., 2003; Abbruzzese and Berardelli, 2006). A major goal in the field is to determine which of these models is correct.

What is known concerning the movement of the BoNTs? BoNT/A and BoNT/E were recently shown to undergo retrograde axonal transport in cultured motor neurons, but putative transfer and action on upstream neurons was not addressed in these in vitro experiments (Restani et al., 2012a). For clarity, we note that these authors used the term "distal" or "central" effects, but this refers to the action of the toxins in the somatodendritic compartment (which can lie in the CNS in vivo) versus their action within pre-synaptic boutons, where they were initially taken up. However, it is well established that the toxin LC can diffuse and cleave SNAREs throughout neurons, so we use the term "distal effects" to indicate the action of the toxins on neurons that are upstream from the neurons that mediate the initial uptake step. Interestingly, in whole-animal experiments, BoNT/A was reported to have bona fide distal effects (i.e., effects on upstream neurons) (Antonucci et al., 2008; Restani et al., 2011)), but this could not be reproduced in an in vitro system based on cultured neurons (Lawrence et al., 2012). Furthermore, the interpretation of data obtained from in vivo approaches can be confounded by myriad variables, including long axon collaterals that can make it appear as if distal effects are occurring. Collectively, the question of whether BoNT/A confers its medicinal effects indirectly (network remodeling) or directly (by interneuronal transfer and action of holotoxin) remains to be definitively addressed. The in vitro system described in the present study circumvents the caveats mentioned earlier and allowed us to resolve the controversy surrounding distal effects of CNTs.

The goal of the present study was to directly ascertain whether CNTs move from neuron to neuron, in an active form, resulting in the cleavage of SNAREs in cells that are upstream from the initial uptake neurons. As earlier work focused on in vivo experiments (Antonucci et al., 2008; Restani et al., 2011, 2012a, 2012b), here, we sought an in vitro experimental approach that can be used to directly visualize toxin action within networks of neurons and that provides an experimentally amenable system to elucidate the mechanisms that mediate local versus distal effects. In our study, we utilized cultured hippocampal neurons, grown in microfluidic devices, to directly compare our results with those of Antonucci et al. (2008), who injected BoNT/A directly into the hippocampus of intact mice. The experiments reported here clearly establish that BoNT/A, BoNT/D, and TeNT undergo retrograde transport along axons, followed by cell-to-cell transfer of the intact holotoxins into upstream neurons where they cleave SNAREs. Additionally, we characterize the receptors and entry pathways that mediate interneuronal transfer of these agents. Together, these experiments demonstrate that CNTs interact with host cells in a more complex manner than was originally envisioned, prompting further re-evaluation of the clinical uses of BoNT/A.

## RESULTS

### Visualization of Interneuronal Transfer and Action of the CNTs

In order to address the question of whether the CNTs move within networks of neurons, we utilized compartmentalized microfluidic devices. Three toxin serotypes were examined: BoNT/A, which cleaves SNAP-25A and -B (hereinafter SNAP-25); and BoNT/D and TeNT, which cleave a number of synaptobrevin (syb) isoforms, with syb2 being the major isoform that mediates rapid exocytosis at many synapses (Montecucco and Schiavo, 1995; Turton et al., 2002; Taylor et al., 2005). The experimental layout is shown in Figure 1A. Rat hippocampal neurons are seeded in one macrochannel (i.e., the soma chamber). By 14 days in vitro, axons project through the microchannels to the opposing macrochamber (i.e., the axon chamber). Dendrites are unable to traverse the microchannel (Figure 1B); hence, only axons are present in the axon chamber (Taylor et al., 2005). The axon chamber was then loaded with a dye, Calcein-AM-green (Figure 1A), to label all of the axons and their corresponding cell bodies and processes residing within the soma chamber. Counterstaining of the soma side with Calcein-AM-red (Figure 1A), which labeled both projecting (to the axonal side) and non-projecting cells, revealed that only 24% ± 1.5% of cells seeded in the soma side extend their axons to the axon chamber (green cells) and that over half of these "projecting neurons" (52% ± 2.9%) reside in the proximal region of the chamber, close to the mouth of the microchannels. With rare exceptions (3% ± 0.6%), neurons distal from the microgroove barrier do not extend axons to the axon chamber, creating a hierarchy of neuronal connectivity. Representative images of distal and proximal regions in the soma side, along with a proximal region in the axon side, are shown in Figure 1A (right panels). Microfluidic isolation is achieved and maintained by keeping the media volume in the soma chamber higher (300 μl), as compared to that
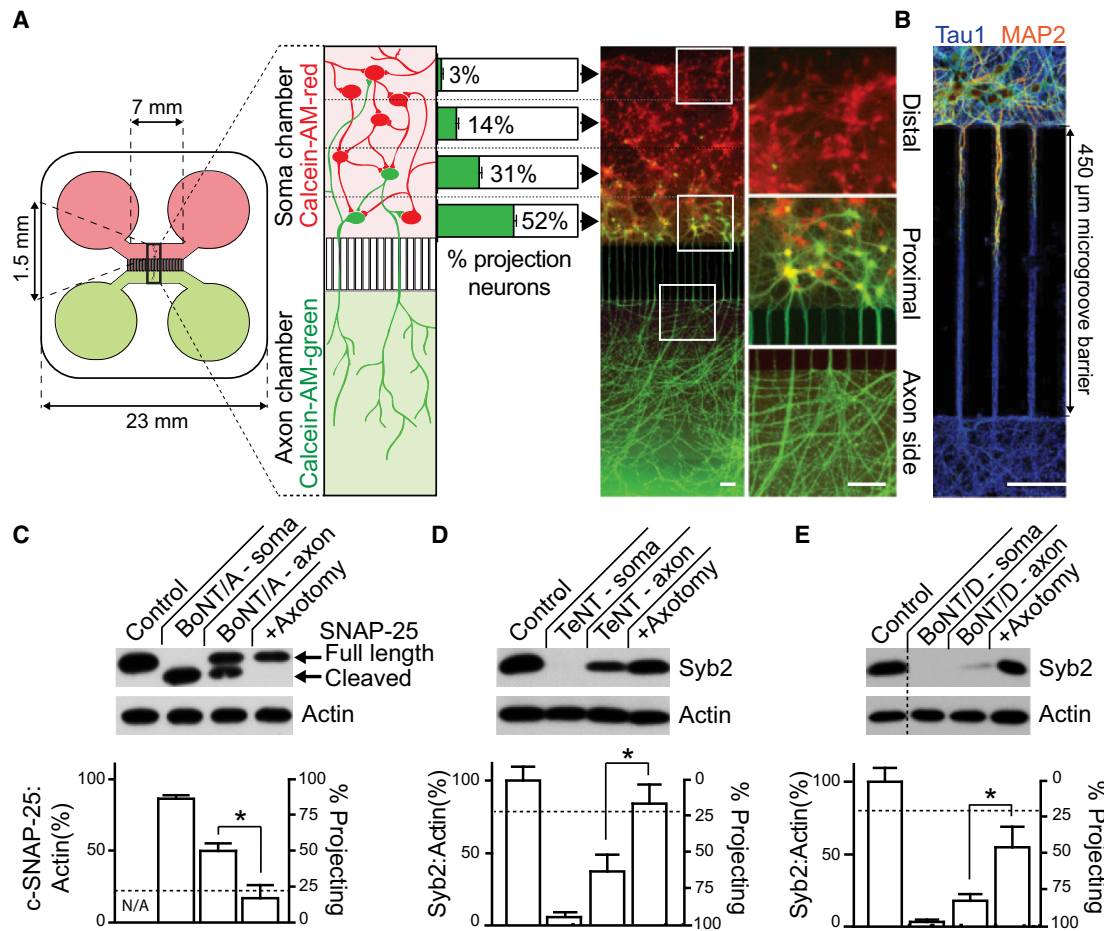
**Figure 1. CNTs Cleave Substrates beyond the Levels Predicted by Connectivity of Neurons in Compartmentalized Microfluidic Devices**

(A) Dissociated hippocampal neurons were seeded into the soma chamber (top, red) of a microfluidic device. The number of cells that extend axons through the microchannels to the axon chamber (projecting cells) was determined by differential Calcein-AM-red and -green staining, added to the soma (top) and axon (bottom) chambers, respectively. Projecting cells are green/yellow; non-projecting cells are red. The number of projecting neurons drops sharply from 52% ± 2.9% of cells residing proximal to the microchannels in the soma side to 31% ± 3.5% in the mid-proximal region, 14% ± 2.5% in the mid-distal region, and to just 3% ± 0.6% in the most distal region. Representative image of Calcein-stained neurons; white boxes denote regions that are magnified in the right panel.

(B) Dendrites fail to reach the axon side due to the length of the microgroove barrier, creating an isolated axonal compartment, as illustrated by staining with MAP2 to mark dendrites (red/orange) and tau1 to mark axons (blue).

(C) BoNT/A was added to the soma (10 nM) or axon (30 nM) side of the microfluidic device. After 48 hr, cells in the soma chamber were assayed for substrate cleavage via immunoblot analysis. The horizontal dotted line represents the total fraction of cells projecting to the axon side (24% ± 1.5%). Cleavage of substrate was abolished by axotomy.

(D and E) Similarly, TeNT (D) or BoNT/D (E) was added to either the soma or axon side of microfluidic devices, and cleavage of syb2 was assayed by immunoblot analysis.

All plotted values are averages ± SEM; experiments were carried out with three to five independent rat litters. Scale bars, 100 μm. *p ≤ 0.05. See also Figures S1 and S2.

in the axon chamber (200 μl). This volume difference prevents diffusion of molecules from the axon side to the soma side, as reported previously (Taylor et al., 2005; Wang et al., 2015; David et al., 2012); fluidic isolation is validated using fluorescent markers in Figure S1. Moreover, we routinely include fluorescent dyes in the microfluidics to ensure that fluidic isolation is maintained and leak does not occur; when leak occurs, these samples are excluded from further analysis (Figure S1; <5% of the devices fail to seal).

When the soma chamber was incubated with BoNT/A, BoNT/D, or TeNT, nearly complete cleavage of SNAP-25 or

syb2, respectively, was observed at 48 hr (Figures 1C–1E). Cleavage of SNAP-25 by BoNT/A was monitored by measuring the ratio of full-length to cleaved protein (c-SNAP-25); actin served as a loading control. Cleavage of syb2 by TeNT and BoNT/D was monitored by measuring the loss of substrate signal, and these values were normalized to the actin signals in each sample. Interestingly, when toxins were added to the axon side, the degree of cleavage observed in the soma side far exceeded the levels predicted by the fraction of neurons that project axons from the soma to the axon side (24% ± 1.5%, as indicated by the dashed line in the bar graphs in Figures

1C–1E). Namely, 48 hr after addition to the axon side, BoNT/A cleaved 49.6% of SNAP-25, while TeNT and BoNT/D cleaved 63.7% and 83.8% of syb2, respectively, on the soma side. Significant substrate protection was observed following axotomy in the axon chamber, demonstrating that axonal transport was required for efficient substrate cleavage in the soma chamber; these observations further rule out diffusion of toxin from one side of the device to the other. While we routinely used 10–30 nM toxin in the axon side, distal effects were also observed using lower, clinically relevant concentrations (picomolar) of BoNT/A and TeNT, though this required an extended incubation period (Figure S2); hence, the remainder of the experiments were carried out using higher toxin concentrations so that we could assay for toxin effects on short timescales (24–48 hr).

Next, we conducted experiments to determine more directly whether the observed substrate cleavage within the soma chamber occurs in second-order neurons that do not project axons to the axon side. Due to the dramatic difference in connectivity of neurons between proximal and distal regions of the soma side, we monitored substrate cleavage in those two regions via immunocytochemistry. For all of these experiments, Calcein-AM-green was added to the axon side to mark projecting neurons; representative images of this staining along with the corresponding immunocytochemistry are shown (Figure 2A). Each microfluidic was stained for MAP2 to mark all neurons and VGlut1 to mark synapses (similar results were obtained using vGAT to mark inhibitory synapses; data not shown). Cleavage of SNAP-25 by BoNT/A was measured using an antibody that is specific for the cleaved form of this protein (c-SNAP-25). Only background signals for c-SNAP-25 were observed, proximally and distally, in control microfluidics, and the greatest degree of cleavage was observed in both regions when the soma chamber was directly treated with BoNT/A; these data are quantified in Figure 2B. We then treated the axon chamber with BoNT/A and observed significant cleavage in the proximal region of the soma side, as expected, since over 50% of cells in this region project to the axon side. Importantly, we also observed efficient cleavage distally, in neurons that did not project axons to the axon side, as evidenced by the absence of Calcein-AM staining. As a control, we again performed axotomy, which diminished the cleavage of SNAP-25.

To determine the generality of the findings obtained using BoNT/A, we tested both TeNT and BoNT/D using a similar experimental design. Representative images of Calcein-AM-green, along with VGlut and syb2 staining for each experiment, are shown (Figures 3A and 3C). In control microfluidics, syb2 and VGlut1 are co-localized, as expected. Soma treatment with TeNT and BoNT/D resulted in near-complete cleavage of syb2 in both the proximal and distal regions, as illustrated by the lack of staining following the application of either toxin, which was quantified in Figures 3B and 3D. Axon-side treatments with either toxin led to efficient cleavage in the soma side, both proximal to, and distal from, the microchannels; cleavage was inhibited by axotomy. Notably, BoNT/D had particularly strong distal effects; we observed almost complete cleavage of its substrate throughout the microfluidic device, including the reservoirs, which are millimeters away (data not shown).

## Holotoxins, Released into the Media from the Initial Uptake Neuron, Enter Upstream Neurons

The aforementioned experiments provide strong support for the idea that a fraction of BoNT/A, BoNT/D, and TeNT can, in fact, undergo retrograde transport and inter-neuronal transfer. In the next series of experiments, we further explored this idea by determining whether substrate cleavage in the soma chamber could be blocked by adding an excess toxin receptor binding ($H_C$) domain, to interfere with toxin-receptor recognition, or by adding anti-toxin antibodies that, in principle, should intercept toxin molecules as they leave the initial uptake neuron, thus preventing their action upon other neurons. Neutralizing anti-BoNT/A and anti-BoNT/D antibodies were tested previously (Björnstad et al., 2014; Kalb et al., 2009); anti-TeNT antibody was validated by neutralization of TeNT in primary hippocampal neurons (data not shown). The scheme for these experiments is shown in Figure 4A.

Holotoxins were added to the axon side, while the soma side was pre-incubated with corresponding $H_C$ fragments, or anti-toxin antibodies. Substrate cleavage in both proximal and distal regions in the soma macrochannel was monitored via immunocytochemistry, as described in Figure 2. For all three toxins, $H_C$ fragments and anti-toxin antibodies provided significant protection from cleavage within the soma side (Figures 4B–4D). In each case, there was a trend toward greater protection in the distal regions, as compared to the proximal regions, but since 48% of neurons in the proximal region do not project axons to the axon side of the device (see Figure 1A), some degree of protection, even in the proximal region, was expected if the toxins underwent interneuronal transfer. Together, these results indicate that, after uptake on the axon side, the toxins are retrogradely transported to the soma side, where they are released into the media; the toxins then enter upstream neurons.

## An Alternative SV-Independent Pathway Underlies the Distal Effects of the CNTs

Following entry into neurons via recycling SVs, acidification of the vesicle lumen triggers the translocation of the LC into the cytosol. In order for the toxin to traffic to the soma side, and to be released in an active form to enter and affect upstream neurons, the LC must remain linked to the HC. This can be achieved if the toxin is located in a non-SV compartment that does not undergo significant luminal acidification (or acidifies slowly enough to first allow transport without translocation). Previous work reported that TeNT, as well as BoNT/A and BoNT/E, indeed share a common retrograde transport organelle that does not acidify (Restani et al., 2012a). However, in contrast to BoNT/A, BoNT/E was shown not to exert distal effects (Restani et al., 2012b; Antonucci et al., 2008), and trafficking of BoNT/D has not been studied.

To directly monitor toxin co-trafficking, $H_C$ fragments derived from each of the three serotypes studied here were labeled with either Alexa Fluor 488 or 568 and added to the axon chamber for 4–24 hr prior to imaging. Entry and trafficking of the labeled $H_C$ fragments were monitored, within the microchannels, ~350–400 μm away from the axon side (Figure 5A, red box). As before, microfluidic isolation was maintained with a higher volume of media on the soma side throughout the entire length of
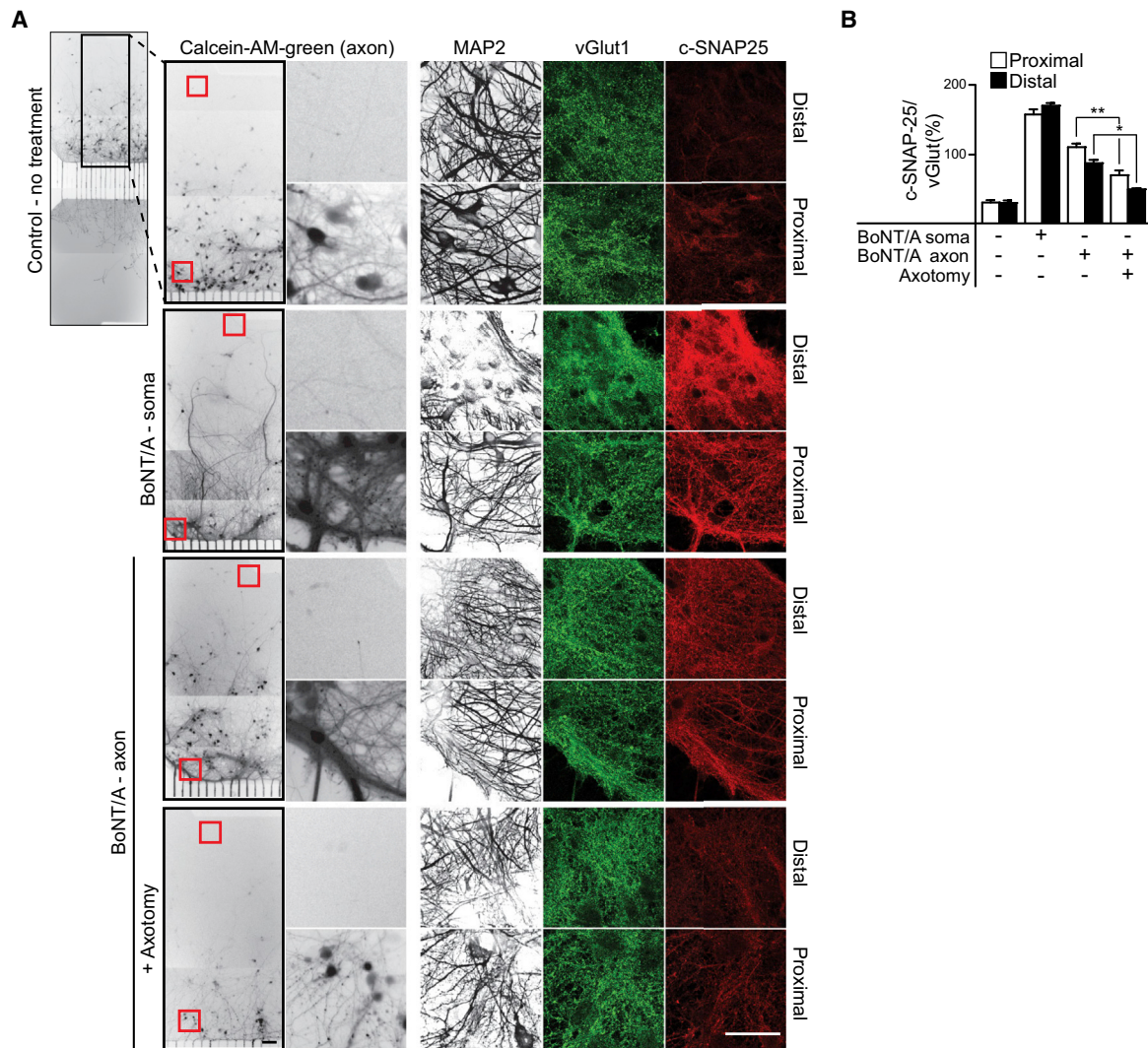
**Figure 2. Cleavage of Substrate by BoNT/A in Upstream Neurons**

(A) Representative Calcein-AM-green staining, after addition of dye to the axon side only, marking projecting neurons; proximal and distal regions of the soma side of the microfluidics are shown (regions of interest indicated by red boxes). Neurons growing in both proximal and distal regions stain positive for the dendritic marker, MAP2, and the synaptic vesicle marker, vGlut1; Calcein-AM and MAP2 images were inverted and switched to grayscale for clarity. Neurons were treated with BoNT/A on the soma side (10 nM) or axon side (30 nM) with and without axotomy for 24 hr. Cleavage of SNAP-25 was assayed using an antibody that recognizes the BoNT/A cleaved form of this protein (c-SNAP-25). Only background signals for c-SNAP-25 were observed, both proximally and distally, in control microfluidics; robust cleavage was observed following soma treatment with BoNT/A, in both regions. After addition of BoNT/A to the axon side, c-SNAP-25 was observed in proximal as well as distal regions of the soma side, and cleavage was significantly reduced by axotomy.

(B) The intensity of c-SNAP-25, normalized to vGlut1 was quantified. The statistical analysis was performed comparing proximal to proximal, or distal to distal, regions.

All plotted values are averages ± SEM; minimum of three to four images from each region (proximal/distal), from four to five separate experiments. Scale bars, 100 μm. *p ≤ 0.05; **p ≤ 0.01.

the experiment to prevent diffusion of the $H_C$ domains to the soma side (see Figure S1). We observed that labeled $H_C$ domains derived from both BoNT/D and BoNT/A (D-$H_C$ and A-$H_C$, respectively) co-localized to the same transport organelles (77%; Figure 5E), which were observed moving retrogradely (Figure 5B). $H_C$ fragments from BoNT/D and TeNT were also co-localized in retrograde transport organelles (80%; Figures 5C and 5E), which do not acidify, as evidenced by a lack of co-localization of D-$H_C$ with LysoTracker (16%; Figures 5D and 5E; Movie S1). These

observations fit the idea that a common carrier mediates the retrograde trafficking of these agents. The lack of acidification allows the holotoxins to remain intact so that when they are released they are able to bind, enter, and affect upstream neurons.

TeNT, BoNT/A, and BoNT/D utilize SV2 as a protein receptor to enter cells via the SV recycling pathway (Dong et al., 2006; Yeh et al., 2010; Mahrhold et al., 2006; Peng et al., 2011). In the absence of this receptor, cleavage of substrate by all three
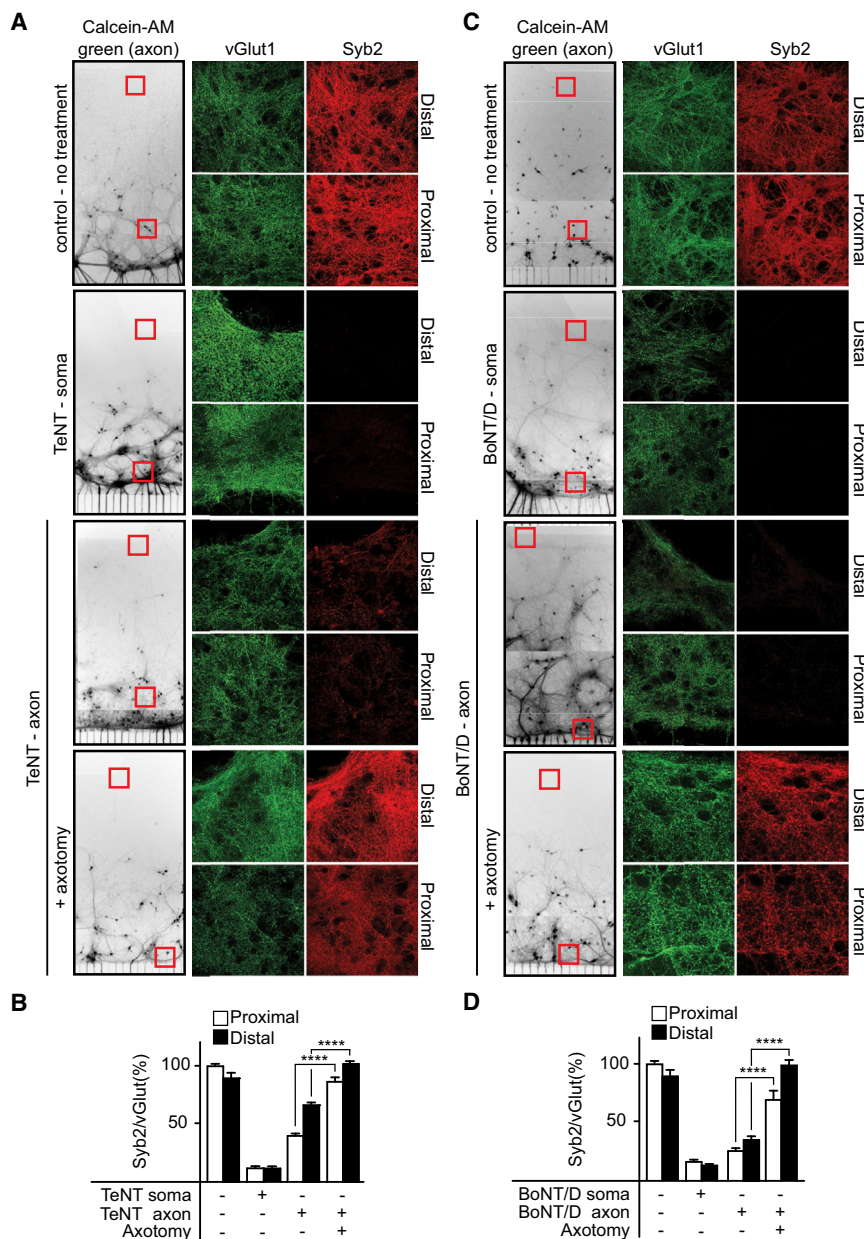
OPEN ACCESS

**Cell**Press



**Figure 3. Cleavage of Substrate by BoNT/D and TeNT in Upstream Neurons**

(A and B) As in Figure 2, (A) images of Calcein-AM-green-stained neurons were inverted and switched to grayscale. Neurons in both proximal and distal regions of the soma side stain positive for the synaptic vesicle marker, vGlut1 (green), and syb2 (red); MAP2 staining is not shown. Microfluidics were treated with either (A) TeNT or (B) BoNT/D for 24 hr (10 nM toxin for soma side treatments, 30 nM for axon side treatments), fixed, and assayed for syb2 cleavage via immunocyto-chemistry. In both cases, cleavage of substrate was observed in proximal as well as distal, non-projecting neurons, and syb2 was protected from cleavage by axotomy.

(C and D) Syb2 signals normalized to vGlut1.

All plotted values are averages ± SEM; minimum of three to four images from each region (proximal/distal), from four to five separate experiments. ****$p \leq 0.0001$.

quantum dots (Qdots) (Figure S3), were added to the axon side of cultures 13–14 DIV (days in vitro). After 6 hr, entry and trafficking of $H_C$ Qdots was monitored, as described earlier for the organic dyes. Qdot-labeled $H_C$ domains derived from all three toxins entered WT axons and underwent retrograde transport toward the soma side (Figures 5F–5K). The speed of toxin $H_C$ transport is in agreement with data from earlier studies of TeNT and BoNT/A (Restani et al., 2012a) and is consistent with the speed reported for fast axon retrograde transport of endosomal carriers (Deinhardt et al., 2006, 2007; Salinas et al., 2009). Importantly, all three $H_C$ fragments efficiently entered SV2A/B DKO neurons, where they also underwent processive, retrograde transport with speeds that were comparable to those found using WT neurons (Figures 5F–5K, right panel; Movie S2). The entry and overlap in speed distribution profiles of these toxin fragments indicate that (1) all three toxins share a retrograde trafficking route and that (2) sorting of the toxin into this organelle is independent of interactions with SV2, clearly establishing the existence of second receptor and uptake pathway for each toxin.

toxins is significantly reduced, and knockout (KO) animals lacking SV2A/B are resistant to the toxins. Of the three isoforms of SV2, the majority of hippocampal neurons exclusively express SV2A and SV2B (Dong et al., 2006; Janz and Südhof, 1999; Bajjalieh et al., 1994; Peng et al., 2011), and only a small population of hippocampal neurons express SV2C (Peng et al., 2011; Dong et al., 2008). Therefore, neurons obtained from SV2A/B double-KO (DKO) animals serve as a desirable model to investigate whether the secondary, "non-productive" pathway (i.e., fails to trigger translocation) occurs via an SV2-independent mechanism. To address this, hippocampal neurons from embryonic day (E)15.5 (wild-type) WT and SV2A/B DKO mice were seeded into microfluidic devices. Toxin $H_C$ fragments, conjugated to

## Assessing Candidate Receptors for the Second CNT Uptake Pathway

Together, the results thus far reveal two distinct uptake/trafficking pathways for BoNT/A, BoNT/D, and TeNT: the canonical SV pathway, which leads to acidification and local effects, and a second, SV receptor independent pathway that routes the toxins to a common non-acidified carrier that mediates delivery to distal
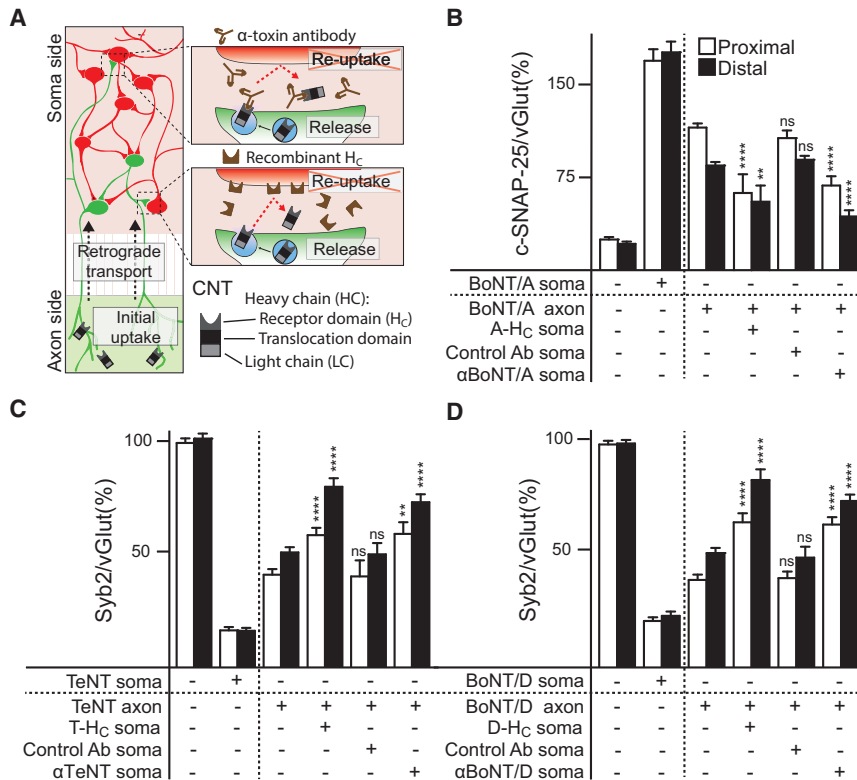
**Figure 4. BoNT/A, BoNT/D, and TeNT Are Released by the Primary Uptake Neurons to Enter Upstream Neurons**

(A–D) In (A), a schematic representation is shown of the experimental design. Soma chambers were pre-treated with either A-H$_C$, D-H$_C$, or T-H$_C$ domains (300 nM for A-H$_C$ and T-H$_C$, 100 nM for D-H$_C$) or anti-CNT antibodies specific for each toxin, followed by addition of holotoxin to the axon side of the microfluidic (30 nM of BoNT/A and TeNT, 10 nM of BoNT/D). After 24 hr, neurons were fixed and stained for VGlut1, MAP2, and c-SNAP-25 for BoNT/A (B), or syb2 for TeNT (C) and BoNT/D (D). Images were obtained from proximal and distal regions of soma side and analyzed as in Figures 2 and 3. In each case, inclusion of H$_C$ fragments, or antibodies, in the soma chamber, protected neurons from substrate cleavage, both proximally and distally, for BoNT/A (B), TeNT (C), and BoNT/D (D), demonstrating that toxins physically leave uptake neurons and enter upstream neurons where they cleave SNAREs.

All plotted values are averages ± SEM; minimum of three to four images from each region (proximal/distal), from four to five separate experiments. **p ≤ 0.01; ****p ≤ 0.0001; ns indicates p > 0.05.

---

sites. As detailed earlier, receptors for the SV pathway have been established for most of the CNTs: SV2 serves as the SV receptor for all three toxins examined here. However, it has also been reported that FGFR3 and nidogens 1 and 2 might serve as receptors for BoNT/A and TeNT, respectively (Bercsenyi et al., 2014; Jacky et al., 2013). Namely, the 2,3 loop of FGFR3b (FGFR3L2,3) was shown to interfere with toxin and host cell interactions (Jacky et al., 2013), and peptides derived from nidogens 1 and 2 (N1 and N2, respectively) were shown to protect mice from the effects of TeNT (Bercsenyi et al., 2014). We tested these reagents in microfluidic devices by pre-incubating them with holotoxins and then adding them to the axon side, followed by immunocytochemistry to determine whether they prevented toxin action in proximal and distal regions in the soma chamber. The scheme for these experiments is shown in Figure 6A.

As a control, and as expected, the A-H$_C$ fragment protected neurons in the soma macrochannel when added together with BoNT/A on the axon side (Figure 6B). Surprisingly, inclusion of the FGFR3L2,3, which was implicated in the action of BoNT/A (Jacky et al., 2013), but not any other serotype, resulted in enhanced cleavage of SNAP-25 in the proximal region of the soma macrochannel and had no significant effect on cleavage in the distal region. Equally surprising was the finding that the nidogen peptide N2 resulted in significant protection of distal neurons from the action of BoNT/A. This was unexpected, as A-H$_C$ was found to bind nidogen 2 KO neurons just as efficiently as WT cells, and nidogens have been implicated only in the action of TeNT (Bercsenyi et al., 2014). The N1 peptide was without effect.

Similar experiments were carried out for TeNT. As expected, partial proximal and strong distal protection was observed on the soma side when the axon side was co-treated with TeNT and T-H$_C$ (labeled H$_C$ domain derived from TeNT) (Figure 6C). FGFR3L2,3 was without effect, but both nidogen peptides, N1 and N2, reduced syb2 cleavage on the soma side in three out of four conditions; the only exception was N1, which failed to protect proximally. Together, these data suggest that nidogens might play a role in TeNT entry into, or trafficking within, the second uptake pathway.

Finally, we carried out the same experiments using BoNT/D, which has the most pronounced distal effects studied so far. While the D-H$_C$ fragment from this serotype resulted in protection from syb2 cleavage in both the proximal and distal regions of the soma channel, none of the putative alternative receptor fragments had any demonstrable effect on the action of this toxin (Figure 6D). We note that none of the alternative receptor fragments affected the interaction of native SV2, from brain detergent extracts, with immobilized H$_C$ fragments derived from all three toxins, indicating that these agents do not interfere with the SV uptake pathway (Figures S4A–S4C). In addition, pre-incubation of toxins with alternative receptor fragments had no effect on toxin-mediated substrate cleavage when applied directly to neurons grown in mass culture (Figures S4D–S4F).

## DISCUSSION

Owing to the opposing clinical presentations of tetanus and botulism, which are associated with rigid and flaccid paralysis, respectively, it has been long assumed that TeNT and BoNTs, once they enter the nervous system at the NMJ, have distinct
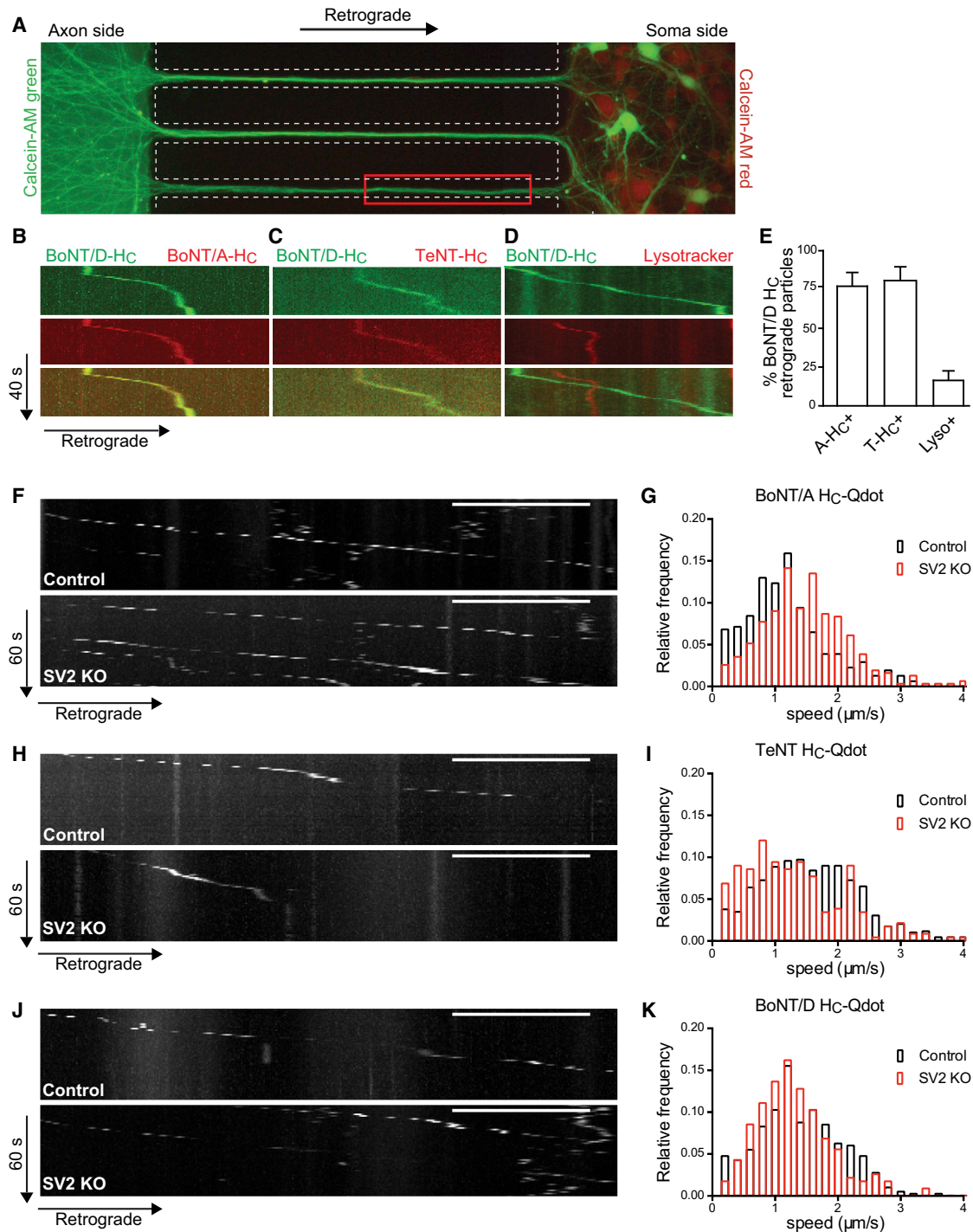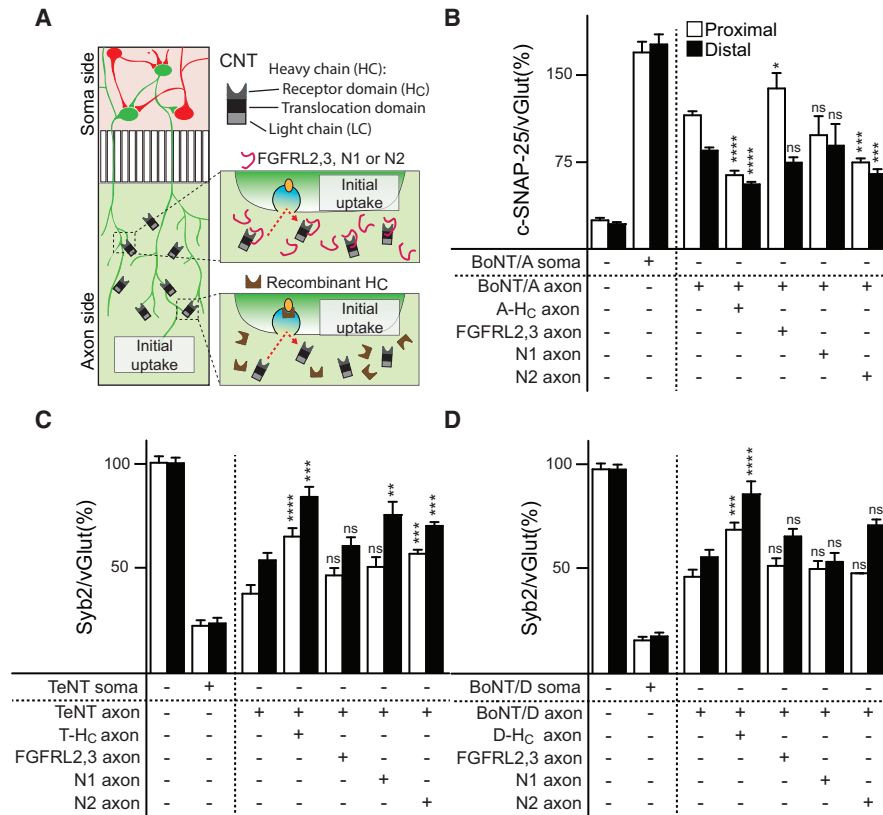
**Figure 5. BoNT/A, TeNT, and BoNT/D Enter Neurons via an SV2-Independent Pathway and Share a Common Transport Organelle**

(A) Overlaid images of Calcein-AM-green added to the axon side with Calcein-AM-red added to the soma side of a microfluidic device. Calcein-AM-green labels all axons, dendrites, and cell bodies of neurons with axons that reached all the way to the axon side of the device. The red box indicates the image acquisition area.

(B–E) Retrograde transport of toxin $H_C$ fragments was visualized using multi-channel live-cell imaging. Representative kymographs show mobile vesicles containing the following Alexa Fluor-labeled-$H_C$ fragments: (B) D-$H_C$ with A-$H_C$ and (C) D-$H_C$ with T-$H_C$. (D) Representative kymograph of axons treated with labeled D-$H_C$ and subsequently loaded with LysoTracker prior to imaging (see also Movie S1). (E) Bar graph depicting average percentage of D-$H_C$-positive organelles undergoing retrograde transport that were also positive for A-$H_C$, T-$H_C$, or LysoTracker. Three to five independent rat litters were used; n = 57–98 particles for D-$H_C$. Values are presented as average ± SEM co-labeled retrograde transport particles.

*(legend continued on next page)*

**Figure 6. Receptor Interference Experiments**

(A–D) In (A), a schematic representation is shown of the experimental design. BoNT/A (30 nM), TeNT (30 nM), and BoNT/D (10 nM) holotoxins were pre-incubated with their respective $H_C$ domains (300 nM for A-$H_C$ and T-$H_C$ and 100 nM for BoNT/D-$H_C$), the FGFRL2,3 receptor fragment (300 nM for BoNT/A and TeNT, and 100 nM for BoNT/D treatments), or N1 or N2 peptide (20 μM) for 60 min prior to being added to the axon side of microfluidic devices. After 24 hr, SNARE cleavage was assayed by immunocytochemistry, as described for Figures 2 and 3.

(B) BoNT/A-mediated cleavage was inhibited by pre-incubation with excess A-$H_C$. Pre-incubation with FGFRL2,3 had no effect on distal cleavage but led to increased proximal cleavage. The N2 peptide protected neurons both proximally and distally, while N1 was without an effect.

(C) TeNT-mediated cleavage was inhibited by pre-incubation of holotoxin with T-$H_C$ and N2. Distal but not proximal protection was also observed with N1, and no effect was seen with the FGFRL2,3 fragment.

(D) D-$H_C$ fragment protected syb2 from cleavage by BoNT/D both proximally and distally; however, none of the remaining fragments tested had any effect on BoNT/D-mediated cleavage.

All plotted values are averages ± SEM; minimum of three to four images from each region (proximal/distal), from four to five independent experiments. *$p \leq 0.05$; **$p \leq 0.01$; ***$p \leq 0.001$; ****$p \leq 0.0001$; ns indicates $p > 0.05$. See also Figure S4.

itineraries. After TeNT is internalized, it is sorted into signaling endosomes that undergo retrograde transport into the spinal cord (Salinas et al., 2010). The holotoxin is then thought to undergo interneuronal transfer to upstream inhibitory neurons to cleave syb2 and block neurotransmission (Deinhardt et al., 2006; von Bartheld, 2004). This disinhibition results in the rigid paralysis characteristic of this agent (Montecucco and Schiavo, 1995; Turton et al., 2002). Since intoxication with BoNTs leads to flaccid paralysis, it was inferred that these toxins remain confined to the NMJ, where they cleave their target SNAREs within presyn-aptic boutons of motor neurons. However, as discussed in the Introduction, recent studies raised the issue that BoNT/A might also undergo transcytosis and cell-to-cell transfer, but this remains controversial. Moreover, there is no evidence that any other BoNTs can move from neuron to neuron to exert distal effects, and numerous questions remain concerning the movement of TeNT from neuron to neuron.

In the present study, we used microfluidic devices to directly address the question of whether BoNT/A and TeNT, as well as the less studied serotype, BoNT/D, can spread within networks

(F–K) In (F, H, and J), representative kymographs show (F) A-$H_C$ Qdot, (H) T-$H_C$ Qdot, and (J) D-$H_C$ Qdot retrograde transport in SV2A$^{-/+}$B$^{-/-}$ and SV2A$^{-/-}$B$^{-/-}$ mouse hippocampal neurons. Scale bars, 10 μm; the total time was 1 min. (G, I, and K) Histograms of instantaneous speed (IS) measured from mobile $H_C$ Qdots. Data were binned at 0.2-μm/s increments by fractional frequency. Black bars are from SV2A$^{-/+}$B$^{-/-}$ mouse (control) neurons, and red bars are from SV2A$^{-/-}$B$^{-/-}$ mouse (SV2DKO) neurons. Two independent mouse litters were used; n > 300 particles for each $H_C$.
*$p \leq 0.05$; **$p \leq 0.01$; ***$p \leq 0.001$; ****$p \leq 0.0001$; ns = $p > 0.05$. See also Figure S3 and Movie S2.
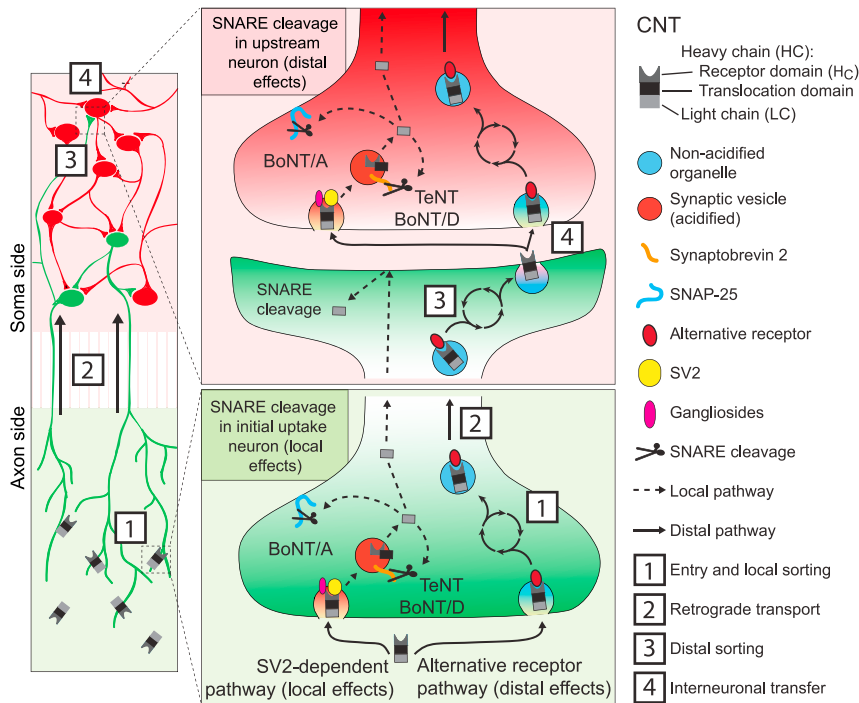
**Figure 7. Model Depicting Two Distinct Trafficking Pathways for BoNT/A, BoNT/D, and TeNT**

Toxins can enter the SV2-dependent pathway, which leads to local effects and results in substrate cleavage throughout the cell (shown in green: pathway indicated by dashed lines, left side), or they can enter via an alternative receptor pathway (solid lines, right side), which leads to distal effects [1]. Since the CNTs tested here do not all enter via the same secondary receptor, additional local sorting steps are required before the CNTs can converge into the common, non-acidified, retrogradely transported organelle [2]. The holotoxin is then delivered to the somato-dendritic compartment, where it undergoes further sorting [3], followed by exocytosis [4]. Holotoxin is then released from the primary uptake neuron and is able to enter a secondary neuron (shown in red) via either pathway: the synaptic vesicle-dependent pathway (by binding SV2), which leads to substrate cleavage, or the synaptic vesicle-independent pathway (by binding to alternative receptor[s]), which leads to further propagation of the holotoxin into upstream neurons.

of neurons to have distal effects (as shown in the model in Figure 7). The microfluidic system used in these experiments provides a straightforward means to analyze toxin action within a hierarchy of neurons, which reflects the connectivity of neuronal networks that exist in vivo. We note that the interpretation of in vivo experiments depends on the absolute knowledge that there are no direct connections between the region injected with toxin and the distal region that is analyzed. This is circumvented in the microfluidics approach by the use of Calcein-AM to precisely map the connectivity of the entire network. Use of this dye made it possible to directly visualize distal effects of the CNTs, as substrate cleavage was observed in neurons that were not directly treated with toxins (Figures 2 and 3). The microfluidics also made it feasible to readily visualize toxin trafficking and to carry out perturbation experiments that cannot be performed in whole-animal studies. For example, it was possible to exploit SV2 KO neurons (as these mice are not viable as adults) to directly reveal the existence of an alternative, SV2-independent uptake pathway of the three toxins examined here.

The retrograde trafficking of TeNT-containing signaling endosomes has been described in detail (Lalli and Schiavo, 2002; Caleo et al., 2009; Deinhardt et al., 2006), but the mechanisms that mediate the sorting and putative transcytosis from the initial uptake neuron to an upstream neuron remain somewhat obscure (Erdmann et al., 1981; Sverdlov and Alekseeva, 1966; Curtis and De Groat, 1968). One of the most convincing observations concerning distal effects of TeNT was the finding, more than 3 decades ago, that the intraspinal injection of TeNT antitoxin, post-peripheral injection of TeNT, prevents hindlimb rigidity in rats (Erdmann et al., 1981). In the present study, we recapitulated these classical findings by showing that inclusion of an

anti-TeNT antibody in the soma chamber of a microfluidic device provides protection from substrate cleavage in secondary neurons. We obtained similar results using the T-H$_C$ fragment. These results directly demonstrate that TeNT physically leaves the primary uptake neuron, is exposed to the extracellular milieu, and then binds and enters another neuron, where it cleaves its substrate. Hence, the reconstitution approach described here made it possible to directly visualize the distal action of TeNT. Parallel experiments using BoNT/A and BoNT/D revealed that both of these serotypes were also intercepted, during interneuronal transfer, by anti-toxin antibodies that prevent entry; protection from substrate cleavage was also observed using H$_C$ fragments. These findings demonstrate that these two serotypes also undergo cell-to-cell transfer to exert distal effects. Whether BoNTs B, C, G, and F spread within networks of neurons is a question that has yet to be explored.

In the entry pathway that results in substrate cleavage, holotoxin is internalized by endocytosed SVs, and re-acidification of the vesicle lumen leads to the irreversible separation of the LC from the HC, as the LC is translocated into the cytosol. The LC is then trapped inside the cell, and cell-to-cell propagation of the holotoxin is no longer possible. Therefore, either entry of the holotoxin into the retrograde pathway must involve sorting away from recycling SVs before they acidify, or the holotoxins are internalized via a distinct pathway. In order to address this issue, we utilized neurons lacking the SV receptor, SV2. If SV2 serves as the only receptor for these toxins, entry would not be observed in the KO cells. However, Qdot-labeled H$_C$ fragments from all three toxins were able to enter SV2 KO neurons, clearly establishing the existence of an alternative, SV2-independent, entry pathway. Moreover, after entry, each of the Qdot-H$_C$ conjugates underwent axonal retrograde trafficking, with speeds consistent with the signaling organelle that, as Schiavo and

co-workers have shown, transports TeNT, BoNT/A, and BoNT/E (Restani et al., 2012a; Deinhardt et al., 2006). Additionally, this organelle does not acidify, thus allowing for long-distance transport of the holotoxin, in the absence of any translocation. We reiterate that BoNT/E undergoes retrograde traffic in the same compartment that transports TeNT, BoNT/A (Restani et al., 2012a), and BoNT/D (Figure 5). However, BoNT/E does not exert distal effects (Antonucci et al., 2008; Restani et al., 2012a). Thus, inclusion in this retrograde transport pathway does not always necessitate interneuronal transfer, a point we return to further below in the subsequent text. We also note that previous work examined retrograde transport of BoNT/A and TeNT in primary motor neurons (Restani et al., 2012a) (trafficking of BoNT/D has not been studied before); the findings reported here extend these observations to central neurons.

The identification of an alternative uptake pathway, independent of recycling SVs, prompts the question of the identity of the receptors that mediate entry into this pathway. FGFR3 and nidogens 1 and 2 have been proposed to serve as alternative receptors for BoNT/A and TeNT, respectively (Jacky et al., 2013; Bercsenyi et al., 2014). Therefore, we made use of the toxin-binding domains of all three of these putative secondary receptor molecules and determined whether these reagents inhibited distal effects in microfluidic devices. We found that the FGFR3 fragment failed to block the distal effects of BoNT/A, indicating that interactions with this receptor are not required for retrograde trafficking or toxin transfer. Surprisingly, a greater degree of cleavage was observed in the proximal region of the soma channel in the presence of the receptor fragment. The reasons for this observation are unclear, but these results suggest that the FGFR3 fragment might enhance entry via recycling SVs, potentially by increasing the avidity of BoNT/A for the SV2-ganglioside co-receptor. The FGFR3 fragment had no discernable effect on the action of either TeNT or BoNT/D. We then turned our attention to the nidogen 1 and 2 peptides (Bercsenyi et al., 2014), which were shown to protect mice from the effects of TeNT. When added, in conjunction with TeNT, to the axon side, protection in the proximal and distal regions of the soma side was observed (the only case where this did not reach significance was for N1 in the proximal region of the soma channel). These findings are consistent with the idea that nidogens play a role in the distal effects of TeNT. Interestingly, the N2 peptide also protected SNAP-25 from cleavage by BoNT/A, proximally and distally, while N1 was without effect. Finally, neither nidogen peptide had any discernable effect on the action of BoNT/D. In conclusion, the CNTs studied here do not all enter the secondary SV2-independent uptake pathway via a single, common, alternative receptor.

While the experiments summarized earlier indicate convergent early sorting immediately following uptake via the secondary pathway, it should also be noted that, after delivery to the somatodendritic compartment, the holotoxins are likely to undergo further sorting and routing to distinct destinations. For example, as mentioned earlier, BoNT/E is co-trafficked with TeNT and BoNT/A in the same organelle toward the soma (Restani et al., 2012a); however, BoNT/E does not exert distal effects (Antonucci et al., 2008), indicating that, once it is delivered to the cell body, it is sorted away from the interneuronal transfer pathway. Similarly,

TeNT and cholera toxin have been reported to undergo co-transport back to the soma, where they are sorted apart from one another to distinct destinations: cholera toxin is trafficked to the Golgi, while TeNT is targeted to the plasma membrane for exocytosis (Schmieg et al., 2014). Putative sorting steps in the somatodendritic compartment are appealing in the context of the CNTs due to the fact that TeNT causes rigid paralysis, while BoNTs cause flaccid paralysis: these toxins might be routed to different release sites to affect distinct constellations of upstream neurons. However, it is also possible that BoNTs, akin to TeNT, can also cause disinhibition in the spinal cord; this might have gone undetected due to efficient inhibition of the NMJ by the same toxin. Electrophysiological recordings from motor neurons in animals challenged with BoNT/A will resolve this issue.

In summary, the experiments described here help to resolve the controversy regarding distal effects of CNTs by directly visualizing the interneuronal transfer and distal action of TeNT and of BoNT/A and BoNT/D in central neurons. An important next step in these studies will be to engineer the toxins so that they are able to enter only the local pathway by mutating binding sites that mediate recognition of the alternative receptor. At present, these efforts can begin by focusing on interactions with nidogens for TeNT, and perhaps for BoNT/A, but this work will await the identification of the secondary receptor for BoNT/D. A key question will be whether such designer toxins are still efficacious in human patients. If so, off-target effects can be avoided; if not, then many of the clinical effects of these agents are, in fact, due to their distal effects, and this will require a re-evaluation of how these toxins are used in human patients.

## EXPERIMENTAL PROCEDURES

### Ethics Statement

All animal care and experiment protocols in this study were conducted under the guidelines set by the NIH *Guide for the Care and Use of Laboratory Animals* handbook. The protocols were reviewed and approved by the Animal Care and Use Committee (ACUC) at the University of Wisconsin, Madison (assurance number: A3368-01).

### Cell Culture

Rat or mouse hippocampal neurons were cultured as described previously (Yeh et al., 2010). Hippocampal neurons were cultured in standard neuron microfluidic devices (SND450, XONA Microfluidics) mounted on glass coverslips, as previously described (Taylor et al., 2005).

### Treatments in Microfluidic Devices

For the experiments shown in Figures 1, 2, and 3, toxins (30 nM) were applied to the axon side; axotomy was performed 2 hr before toxin treatment by rapid aspiration and reperfusion of the axon chamber. Calcein-AM-red or -green, was added to either side of the microfluidic devices at a final concentration of 1 μM; when treating the axon side, dye was incubated for 5 hr before imaging to allow the entire cell to become stained.

For the experiments shown in Figure 4, A-H$_C$ (300 nM), T-H$_C$ (300 nM), D-H$_C$ (100 nM), control antibody, and anti-toxin antibodies were premixed as specified in the Figure 4 legend and added to the soma side prior to the axon treatment with, respectively, BoNT/A (30 nM), TeNT (30 nM), or BoNT/D (10 nM). For the experiments shown in Figure 6, toxins were premixed with either their respective H$_C$ fragments or FGFR3bL2,3 (300 nM for BoNT/A and TeNT, and 100 nM for BoNT/D), or nidogen N1 or N2 peptides (20 μM each), incubated for 60 min at 37°C, and then added to the axon side. After 24 hr, substrate cleavage was measured via immunocytochemistry.

For soma-side toxin treatments, neurons seeded on the soma side of a microfluidic device were incubated with 10 nM of BoNT/A, BoNT/D, or TeNT for 48 hr (for immunoblotting in Figure 1) or 24 hr (for immunocytochemistry in Figures 2, 3, 4, and 6).

For all treatments, preconditioned media were removed from the microfluidic chamber, mixed with an equal volume of fresh media, and used in the treatments to follow. All control microfluidics were sham treated with preconditioned media.

The fraction of neurons that project to the axon side (Figures 1 and S2) was calculated using data from 20 separate chambers obtained from five independent litters of rats.

### Statistical Methods

Statistical significance was by determined by performing the Student's t test for all immunocytochemistry data analysis: ns = $p > 0.05$, *$p \leq 0.05$, **$p \leq 0.01$, ***$p \leq 0.001$, and ****$p \leq 0.0001$. An ANOVA with Dunnett's post hoc test was used to analyze and compare immunoblot data, where $p < 0.05$.

### SUPPLEMENTAL INFORMATION

Supplemental Information includes Supplemental Experimental Procedures, four figures, and two movies and can be found with this article online at http://dx.doi.org/10.1016/j.celrep.2016.06.104.

### REFERENCES

Abbruzzese, G., and Berardelli, A. (2006). Neurophysiological effects of botulinum toxin type A. Neurotox. Res. 9, 109–114.

Antonucci, F., Rossi, C., Gianfranceschi, L., Rossetto, O., and Caleo, M. (2008). Long-distance retrograde effects of botulinum neurotoxin A. J. Neurosci. 28, 3689–3696.

Aymard, C., Giboin, L.S., Lackmy-Vallée, A., and Marchand-Pauvert, V. (2013). Spinal plasticity in stroke patients after botulinum neurotoxin A injection in ankle plantar flexors. Physiol. Rep. 1, e00173.

Bajjalieh, S.M., Frantz, G.D., Weimann, J.M., McConnell, S.K., and Scheller, R.H. (1994). Differential expression of synaptic vesicle protein 2 (SV2) isoforms. J. Neurosci. 14, 5223–5235.

Benoit, R.M., Frey, D., Hilbert, M., Kevenaar, J.T., Wieser, M.M., Stirnimann, C.U., McMillan, D., Ceska, T., Lebon, F., Jaussi, R., et al. (2014). Structural basis for recognition of synaptic vesicle protein 2C by botulinum neurotoxin A. Nature 505, 108–111.

Berardelli, A., and Curra, A. (2002). Effects of botulinum toxin type A on central nervous system function. Naunyn Schmiedebergs Arch. Pharmacol. 365, R50.

Bercsenyi, K., Schmieg, N., Bryson, J.B., Wallace, M., Caccin, P., Golding, M., Zanotti, G., Greensmith, L., Nischt, R., and Schiavo, G. (2014). Tetanus toxin entry. Nidogens are therapeutic targets for the prevention of tetanus. Science 346, 1118–1123.

Björnstad, K., Tevell Åberg, A., Kalb, S.R., Wang, D., Barr, J.R., Bondesson, U., and Hedeland, M. (2014). Validation of the Endopep-MS method for qualitative detection of active botulinum neurotoxins in human and chicken serum. Anal. Bioanal. Chem. 406, 7149–7161.

Boroojerdi, B., Cohen, L.G., and Hallett, M. (2003). Effects of botulinum toxin on motor system excitability in patients with writer's cramp. Neurology 61, 1546–1550.

Caleo, M., Antonucci, F., Restani, L., and Mazzocchio, R. (2009). A reappraisal of the central effects of botulinum neurotoxin type A: by what mechanism? J. Neurochem. 109, 15–24.

Ceballos-Baumann, A.O., Sheean, G., Passingham, R.E., Marsden, C.D., and Brooks, D.J. (1997). Botulinum toxin does not reverse the cortical dysfunction associated with writer's cramp. A PET study. Brain 120, 571–582.

Currà, A., Trompetto, C., Abbruzzese, G., and Berardelli, A. (2004). Central effects of botulinum toxin type A: evidence and supposition. Mov. Disord. 19 (Suppl 8), S60–S64.

Curtis, D.R., and De Groat, W.C. (1968). Tetanus toxin and spinal inhibition. Brain Res. 10, 208–212.

David, A.T., Saied, A., Charles, A., Subramanian, R., Chouljenko, V.N., and Kousoulas, K.G. (2012). A herpes simplex virus 1 (McKrae) mutant lacking the glycoprotein K gene is unable to infect via neuronal axons and egress from neuronal cell bodies. mBio 3, e00144–e12.

de Maio, M. (2008). Therapeutic uses of botulinum toxin: from facial palsy to autonomic disorders. Expert Opin. Biol. Ther. 8, 791–798.

Deinhardt, K., Salinas, S., Verastegui, C., Watson, R., Worth, D., Hanrahan, S., Bucci, C., and Schiavo, G. (2006). Rab5 and Rab7 control endocytic sorting along the axonal retrograde transport pathway. Neuron 52, 293–305.

Deinhardt, K., Reversi, A., Berninghausen, O., Hopkins, C.R., and Schiavo, G. (2007). Neurotrophins Redirect p75NTR from a clathrin-independent to a clathrin-dependent endocytic pathway coupled to axonal transport. Traffic 8, 1736–1749.

Dong, M., Richards, D.A., Goodnough, M.C., Tepp, W.H., Johnson, E.A., and Chapman, E.R. (2003). Synaptotagmins I and II mediate entry of botulinum neurotoxin B into cells. J. Cell Biol. 162, 1293–1303.

Dong, M., Yeh, F., Tepp, W.H., Dean, C., Johnson, E.A., Janz, R., and Chapman, E.R. (2006). SV2 is the protein receptor for botulinum neurotoxin A. Science 312, 592–596.

Dong, M., Liu, H., Tepp, W.H., Johnson, E.A., Janz, R., and Chapman, E.R. (2008). Glycosylated SV2A and SV2B mediate the entry of botulinum neurotoxin E into neurons. Mol. Biol. Cell 19, 5226–5237.

Erdmann, G., Hanauske, A., and Wellhöner, H.H. (1981). Intraspinal distribution and reaction in the grey matter with tetanus toxin of intracisternally injected anti-tetanus toxoid F(ab')2 fragments. Brain Res. 211, 367–377.

Fischer, A. (2013). Synchronized chaperone function of botulinum neurotoxin domains mediates light chain translocation into neurons. Curr. Top. Microbiol. Immunol. 364, 115–137.

Foster, L., Clapp, L., Erickson, M., and Jabbari, B. (2001). Botulinum toxin A and chronic low back pain: a randomized, double-blind study. Neurology 56, 1290–1293.

Fu, F.N., Busath, D.D., and Singh, B.R. (2002). Spectroscopic analysis of low pH and lipid-induced structural changes in type A botulinum neurotoxin relevant to membrane channel formation and translocation. Biophys. Chem. 99, 17–29.

Fu, Z., Chen, C., Barbieri, J.T., Kim, J.J.P., and Baldwin, M.R. (2009). Glycosylated SV2 and gangliosides as dual receptors for botulinum neurotoxin serotype F. Biochemistry 48, 5631–5641.

Galloux, M., Vitrac, H., Montagner, C., Raffestin, S., Popoff, M.R., Chenal, A., Forge, V., and Gillet, D. (2008). Membrane Interaction of botulinum neurotoxin A translocation (T) domain. The belt region is a regulatory loop for membrane interaction. J. Biol. Chem. 283, 27668–27676.

Giladi, N. (1997). The mechanism of action of botulinum toxin type A in focal dystonia is most probably through its dual effect on efferent (motor) and afferent pathways at the injected site. J. Neurol. Sci. 152, 132–135.

Gilio, F., Currà, A., Lorenzano, C., Modugno, N., Manfredi, M., and Berardelli, A. (2000). Effects of botulinum toxin type A on intracortical inhibition in patients with dystonia. Ann. Neurol. 48, 20–26.

Gill, D.M. (1982). Bacterial toxins: a table of lethal amounts. Microbiol. Rev. 46, 86–94.

Jacky, B.P., Garay, P.E., Dupuy, J., Nelson, J.B., Cai, B., Molina, Y., Wang, J., Steward, L.E., Broide, R.S., Francis, J., et al. (2013). Identification of fibroblast growth factor receptor 3 (FGFR3) as a protein receptor for botulinum neurotoxin serotype A (BoNT/A). PLoS Pathog. 9, e1003369.

Jahn, R., and Niemann, H. (1994). Molecular mechanisms of clostridial neurotoxins. Ann. N Y Acad. Sci. 733, 245–255.

Jankovic, J. (1994). Botulinum toxin in movement disorders. Curr. Opin. Neurol. 7, 358–366.

Janz, R., and Südhof, T.C. (1999). SV2C is a synaptic vesicle protein with an unusually restricted localization: anatomy of a synaptic vesicle protein family. Neuroscience 94, 1279–1290.

Kalb, S.R., Lou, J., Garcia-Rodriguez, C., Geren, I.N., Smith, T.J., Moura, H., Marks, J.D., Smith, L.A., Pirkle, J.L., and Barr, J.R. (2009). Extraction and inhibition of enzymatic activity of botulinum neurotoxins/A1, /A2, and /A3 by a panel of monoclonal anti-BoNT/A antibodies. PLoS ONE 4, e5355.

Lalli, G., and Schiavo, G. (2002). Analysis of retrograde transport in motor neurons reveals common endocytic carriers for tetanus toxin and neurotrophin receptor p75NTR. J. Cell Biol. 156, 233–239.

Lawrence, G.W., Ovsepian, S.V., Wang, J., Aoki, K.R., and Dolly, J.O. (2012). Extravesicular intraneuronal migration of internalized botulinum neurotoxins without detectable inhibition of distal neurotransmission. Biochem. J. 441, 443–452.

Mahrhold, S., Rummel, A., Bigalke, H., Davletov, B., and Binz, T. (2006). The synaptic vesicle protein 2C mediates the uptake of botulinum neurotoxin A into phrenic nerves. FEBS Lett. 580, 2011–2014.

Mahrhold, S., Strotmeier, J., Garcia-Rodriguez, C., Lou, J., Marks, J.D., Rummel, A., and Binz, T. (2013). Identification of the SV2 protein receptor-binding site of botulinum neurotoxin type E. Biochem. J. 453, 37–47.

Marchand-Pauvert, V., Aymard, C., Giboin, L.S., Dominici, F., Rossi, A., and Mazzocchio, R. (2013). Beyond muscular effects: depression of spinal recurrent inhibition after botulinum neurotoxin A. J. Physiol. 591, 1017–1029.

Montal, M. (2010). Botulinum neurotoxin: a marvel of protein design. Annu. Rev. Biochem. 79, 591–617.

Montecucco, C., and Schiavo, G. (1995). Structure and function of tetanus and botulinum neurotoxins. Q. Rev. Biophys. 28, 423–472.

Nishiki, T., Kamata, Y., Nemoto, Y., Omori, A., Ito, T., Takahashi, M., and Kozaki, S. (1994). Identification of protein receptor for Clostridium botulinum type B neurotoxin in rat brain synaptosomes. J. Biol. Chem. 269, 10498–10503.

Peng, L., Tepp, W.H., Johnson, E.A., and Dong, M. (2011). Botulinum neurotoxin D uses synaptic vesicle protein SV2 and gangliosides as receptors. PLoS Pathog. 7, e1002008.

Peng, L., Berntsson, R.P., Tepp, W.H., Pitkin, R.M., Johnson, E.A., Stenmark, P., and Dong, M. (2012). Botulinum neurotoxin D-C uses synaptotagmin I and II

as receptors, and human synaptotagmin II is not an effective receptor for type B, D-C and G toxins. J. Cell Sci. 125, 3233–3242.

Pirazzini, M., Henke, T., Rossetto, O., Mahrhold, S., Krez, N., Rummel, A., Montecucco, C., and Binz, T. (2013). Neutralisation of specific surface carboxylates speeds up translocation of botulinum neurotoxin type B enzymatic domain. FEBS Lett. 587, 3831–3836.

Popoff, M.R., and Bouvet, P. (2013). Genetic characteristics of toxigenic Clostridia and toxin gene evolution. Toxicon 75, 63–89.

Priori, A., Berardelli, A., Mercuri, B., and Manfredi, M. (1995). Physiological effects produced by botulinum toxin treatment of upper limb dystonia. Changes in reciprocal inhibition between forearm muscles. Brain 118, 801–807.

Puhar, A., Johnson, E.A., Rossetto, O., and Montecucco, C. (2004). Comparison of the pH-induced conformational change of different clostridial neurotoxins. Biochem. Biophys. Res. Commun. 319, 66–71.

Restani, L., Antonucci, F., Gianfranceschi, L., Rossi, C., Rossetto, O., and Caleo, M. (2011). Evidence for anterograde transport and transcytosis of botulinum neurotoxin A (BoNT/A). J. Neurosci. 31, 15650–15659.

Restani, L., Giribaldi, F., Manich, M., Bercsenyi, K., Menendez, G., Rossetto, O., Caleo, M., and Schiavo, G. (2012a). Botulinum neurotoxins A and E undergo retrograde axonal transport in primary motor neurons. PLoS Pathog. 8, e1003087.

Restani, L., Novelli, E., Bottari, D., Leone, P., Barone, I., Galli-Resta, L., Strettoi, E., and Caleo, M. (2012b). Botulinum neurotoxin A impairs neurotransmission following retrograde transsynaptic transport. Traffic 13, 1083–1089.

Rossetto, O., Pirazzini, M., and Montecucco, C. (2014). Botulinum neurotoxins: genetic, structural and mechanistic insights. Nat. Rev. Microbiol. 12, 535–549.

Rothman, J.E. (1994). Intracellular membrane fusion. Adv. Second Messenger Phosphoprotein Res. 29, 81–96.

Rummel, A., Eichner, T., Weil, T., Karnath, T., Gutcaits, A., Mahrhold, S., Sandhoff, K., Proia, R.L., Acharya, K.R., Bigalke, H., and Binz, T. (2007). Identification of the protein receptor binding site of botulinum neurotoxins B and G proves the double-receptor concept. Proc. Natl. Acad. Sci. USA 104, 359–364.

Rummel, A., Häfner, K., Mahrhold, S., Darashchonak, N., Holt, M., Jahn, R., Beermann, S., Karnath, T., Bigalke, H., and Binz, T. (2009). Botulinum neurotoxins C, E and F bind gangliosides via a conserved binding site prior to stimulation-dependent uptake with botulinum neurotoxin F utilising the three isoforms of SV2 as second receptor. J. Neurochem. 110, 1942–1954.

Salinas, S., Bilsland, L.G., Henaff, D., Weston, A.E., Keriel, A., Schiavo, G., and Kremer, E.J. (2009). CAR-associated vesicular transport of an adenovirus in motor neuron axons. PLoS Pathog. 5, e1000442.

Salinas, S., Schiavo, G., and Kremer, E.J. (2010). A hitchhiker's guide to the nervous system: the complex journey of viruses and toxins. Nat. Rev. Microbiol. 8, 645–655.

Schantz, E.J., and Johnson, E.A. (1992). Properties and use of botulinum toxin and other microbial neurotoxins in medicine. Microbiol. Rev. 56, 80–99.

Schiavo, G., Matteoli, M., and Montecucco, C. (2000). Neurotoxins affecting neuroexocytosis. Physiol. Rev. 80, 717–766.

Schmieg, N., Menendez, G., Schiavo, G., and Terenzio, M. (2014). Signalling endosomes in axonal transport: travel updates on the molecular highway. Semin. Cell Dev. Biol. 27, 32–43.

Scott, A.B. (1980). Botulinum toxin injection into extraocular muscles as an alternative to strabismus surgery. J. Pediatr. Ophthalmol. Strabismus 17, 21–25.

Silberstein, S., Mathew, N., Saper, J., and Jenkins, S.; for the BOTOX Migraine Clinical Research Group (2000). Botulinum toxin type A as a migraine preventive treatment. Headache 40, 445–450.

Sun, S., Suresh, S., Liu, H., Tepp, W.H., Johnson, E.A., Edwardson, J.M., and Chapman, E.R. (2011). Receptor binding enables botulinum neurotoxin B to sense low pH for translocation channel assembly. Cell Host Microbe 10, 237–247.

Sverdlov, Y.S., and Alekseeva, V.I. (1966). Effect of tetanus toxin on presynaptic inhibition in the spinal cord. Fed. Proc. Transl. Suppl. 25, 931–936.

Taylor, A.M., Blurton-Jones, M., Rhee, S.W., Cribbs, D.H., Cotman, C.W., and Jeon, N.L. (2005). A microfluidic culture platform for CNS axonal injury, regeneration and transport. Nat. Methods 2, 599–605.

Turton, K., Chaddock, J.A., and Acharya, K.R. (2002). Botulinum and tetanus neurotoxins: structure, function and therapeutic utility. Trends Biochem. Sci. 27, 552–558.

von Bartheld, C.S. (2004). Axonal transport and neuronal transcytosis of trophic factors, tracers, and pathogens. J. Neurobiol. 58, 295–314.

Wang, T., Martin, S., Papadopulos, A., Harper, C.B., Mavlyutov, T.A., Niranjan, D., Glass, N.R., Cooper-White, J.J., Sibarita, J.B., Choquet, D., et al. (2015).

Control of autophagosome axonal retrograde flux by presynaptic activity unveiled using botulinum neurotoxin type a. J. Neurosci. 35, 6179–6194.

Williamson, L.C., and Neale, E.A. (1994). Bafilomycin A1 inhibits the action of tetanus toxin in spinal cord neurons in cell culture. J. Neurochem. 63, 2342–2345.

Yao, G., Zhang, S., Mahrhold, S., Lam, K.H., Stern, D., Bagramyan, K., Perry, K., Kalkum, M., Rummel, A., Dong, M., and Jin, R. (2016). N-linked glycosylation of SV2 is required for binding and uptake of botulinum neurotoxin A. Nat. Struct. Mol. Biol. 23, 656–662.

Yeh, F.L., Dong, M., Yao, J., Tepp, W.H., Lin, G., Johnson, E.A., and Chapman, E.R. (2010). SV2 mediates entry of tetanus neurotoxin into central neurons. PLoS Pathog. 6, e1001207.